

# Geometric Control of Chemically Nano-patterned Substrates for Feature Multiplication Using Directed Self-Assembly of Block Copolymers

Paulina A. Rincon Delgadillo<sup>a,b</sup>, Roel Gronheid<sup>b</sup>, Christopher J. Thode<sup>a</sup>, Hengpeng Wu<sup>c</sup>, Yi Cao<sup>c</sup>, Guanyang Lin<sup>c</sup>, Mark Somervell<sup>d</sup>, Kathleen Nafus<sup>d</sup> and Paul F. Nealey<sup>a\*</sup>

<sup>a</sup>Department of Chemical and Biological Engineering, University of Wisconsin – Madison  
1415 Engineering Drive, Madison, WI 53706-1691  
\*nealey@engr.wisc.edu

<sup>b</sup>IMEC, Kapeldreef 75, B-3001 Leuven, Belgium

<sup>c</sup>AZ Electronic Materials, 70 Meister Avenue, Branchburg, NJ 08876-3440

<sup>d</sup>Tokyo Electron America, 2400 Grove Boulevard, Austin, TX 78741

In this study, directed self-assembly of block copolymers (BCP) was investigated as a function of the dimensions of the alternating stripes on chemically nano-patterned substrates, at a constant pattern pitch. It was shown that alignment of the block copolymer with the chemical pattern depends on the width of the guiding stripe. Also, when the ratio of this parameter over the natural periodicity of the BCP ( $W/L_0$ ) is around 0.6, a high degree of perfection is achieved. Finally, the formulation of the BCP was found to impact the process window, as three batches with the same  $L_0$ , presented good alignment at different conditions.

**Keywords:** directed self-assembly, chemo-epitaxy, block copolymer

## 1. Introduction

The use of directed self-assembly (DSA) of block copolymers (BCP) as a means to obtain diverse morphologies and dimensions of interest for lithographic applications, has recently gained an unprecedented impulse from the industry.[1] Even more, the implementation of different chemo-epitaxy flows in a 300mm process to generate lines and spaces of 14nm and below, has brought this technology closer to high volume manufacture.[2, 3] Initial results using feature multiplication show a high degree of perfection of the aligned BCP structures over a wide range of conditions.[4] However, a detailed characterization of the nano-patterned substrates, materials, and process conditions is still necessary in order to understand the critical parameters for DSA of BCP and, therefore, establish a process window for this technique.

In chemo-epitaxy, the chemistry and geometry of the alternating stripes on the chemical

patterns dictate the minimum free energy state and the probability of defect formation.[5, 6] The local composition of the chemically nano-patterned substrates, defined by the materials, must provide sufficient contrast to guide the assembly.[7] The geometry will depend on the process conditions, i.e. exposure and etching. The pre-pattern pitch ( $L_s$ ) must be an approximate multiple of the BCP natural periodicity ( $L_0$ ), to minimize any incommensurability effects.[3, 8] Additionally, theoretical and experimental work has shown that, for feature multiplication, the width of the guiding stripe,  $W$ , may induce the formation of three-dimensional structures throughout the film thickness.[7, 9, 10] A value of  $W=0.6L_0$  has been proposed to be large enough to guide the BCP while obtaining perpendicular domains from the substrate to the free surface.

In this work, DSA of BCP on chemical patterns of diverse geometries is reported. Using standard production tools, control of the critical

dimension (CD) of the pre-patterns through the wafer becomes possible. With a defined chemistry and a constant pitch, the CD of the pre-pattern was varied in order to study the ability of the BCP to accommodate diverse conditions.

## 2. Method

### 2.1 Materials

Cross-linkable polystyrene (XPS, AZEMBLY™ NLD128), hydroxyl-terminated poly(styrene-random-methyl methacrylate) brush (P(S-*r*-MMA)OH, AZEMBLY™ NLD127), and poly(styrene-block-methyl methacrylate) BCP with  $L_o = 28\text{nm}$  (PS-*b*-PMMA, AZEMBLY™ PME312, AZEMBLY™ PME120, AZEMBLY™ PME252), were synthesized by AZ Electronic Materials and used as received. Photoresist AIM5484, was purchased from JSR Micro. Organic solvents RER600 and Orgasolv® STR 301 were purchased from Fujifilm and BASF, respectively, and used as received.

### 2.2 Process

Chemically nano-patterned substrates were prepared at imec on a TEL CLEAN TRACK ACT™12 system, as described previously[2, 11]. Briefly, the DSA dedicated reticle includes a variety of CDs that can be analyzed in a single exposure. For a 3X feature multiplication factor, an 84nm pitch was targeted. Exposures were done on an ASML XT:1900Gi scanner at 1.35NA using quadrupole illumination (XY polarized,  $NA=1.35$ ,  $\sigma_o=0.87$ ,  $\sigma_i=0.72$ ). An inorganic antireflective coating (ARC) film of SiN, of 15nm, was deposited via chemical vapor deposition (CVD) on 300mm Si wafers. The X-PS film, with thickness of 7-8nm, was spun and annealed for 90min at 250°C under a N<sub>2</sub> atmosphere. After resist coating and exposure using vendor recommended settings for post-apply bake (PAB), post-exposure bake (PEB), and development, lines and spaces of 84nm pitch and 35nm critical dimension (CD) were obtained. The samples were submitted to an O<sub>2</sub> and Cl<sub>2</sub> plasma etch step to trim the resist and remove the XPS exposed to the plasma, followed by a wet resist strip using Orgasolv® STR 301. The P(S-*r*-MMA)-OH brush was spun and annealed for 5min at 250°C in a N<sub>2</sub> atmosphere. Non-reacted material was rinsed with RER600. The PS-*b*-PMMA BCP (AZEMBLY™ PME312) was coated on the chemical patterns and annealed with the same process conditions used for deposition of the random brush. For a comparison between three BCP batches, AZEMBLY™ PME120 and

AZEMBLY™ PME252 were used and processed in the same manner.

### 2.3 Characterization

Film thickness of the BCP was measured using a KLA Tencor, SCD100 ellipsometer on 49 points across the wafer's diameter. A Hitachi CG4000 scanning electron microscope (SEM) was used to image and measure the CD of the photoresist after exposure and after trim etch steps, as well as the BCP self-assembled structures.

## 3. Results and discussion

The process followed for sample preparation, implemented at imec, is shown in Figure 1, where the two steps that define the geometry of the chemical patterns are indicated as steps b) and c).[2]

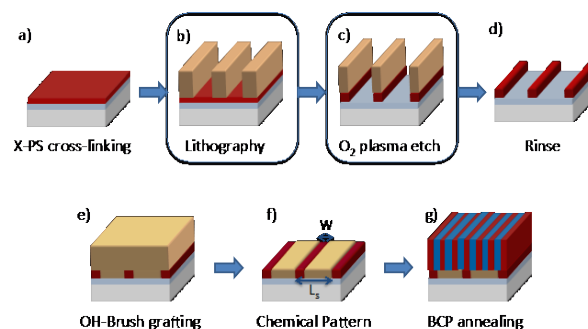


Figure 1. Fabrication of chemically nano-patterned substrates.

The impact of  $w$ , Figure 1f), was investigated by inspecting 8 different CDs (between 0.3 to 0.5 $L_s$  at mask level) at 5 exposure doses. After lithography and development, the CD range of the photoresist was 30.1-42.8nm. Subsequent trim etch, decreased it to 9.4-28.8nm. The non-uniform etching of the resist lines causes the significant variation in the CD range. The wider lines lose less material while the thinner structures tend to etch faster, as shown in Figure 2. Additionally, radial effects during the etching process can be observed in the non-monotonic decrease of the difference between the two CDs. This result suggests that although the initial CD dictates the etching rate of the resist structures, further optimization of the etching process is needed to improve uniformity across the wafer. Due to the lack of contrast between the XPS guiding stripe and the backfill brush, Figure 3, the dimensions of these two regions cannot be measured once the brush is grafted. Therefore, for this study, the obtained SEM values of the CD after trim etch will be assumed to be equal to  $w$ .

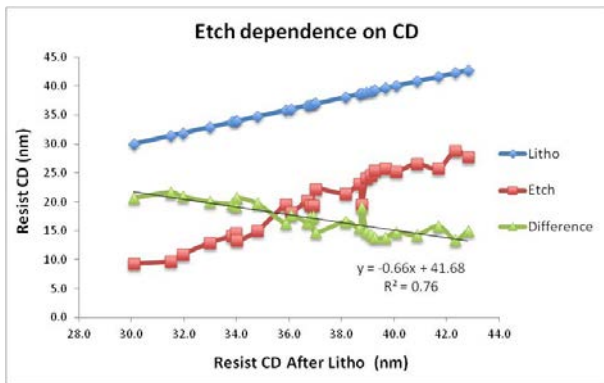


Figure 2. Etching dependence on the initial photoresist CD.

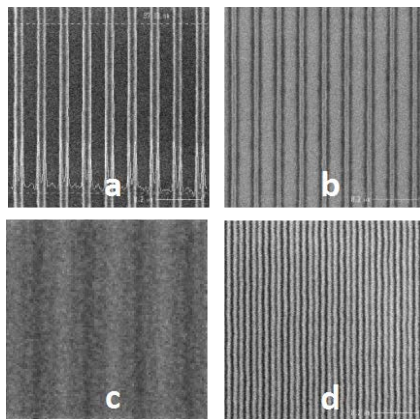


Figure 3. SEM images of chemical pattern fabrication. Steps a) resist after lithography, b) resist after trim etch, c) chemical pattern (different scale), and d) BCP assembly after PMMA removal.

The remaining resist is rinsed with Orgasolv® STR 301 and XPS guiding stripes are obtained. After brush coat, anneal and rinse off the excess material, a 40nm film of BCP was spun on the wafer and annealed. The PMMA block was removed using a dry etch process to improve contrast during SEM inspection. Images were taken at high magnification, covering an area of 0.81mm<sup>2</sup>/image. In order to quantify the quality of the alignment, scores from 0-3 were assigned to each image. Fingerprint-like structures, or lack of order received a 0 score, while a high degree of perfection (absence of defects) obtained 3. Intermediate states were defined as 1 and 2, as shown in Figure 4.

Using this convention, we evaluated the BCP assembly for different conditions, as shown in Figure 5. A wide range of CDs resulted in a high degree of perfection of the domains. The smallest CD measurement after trim etch that generated

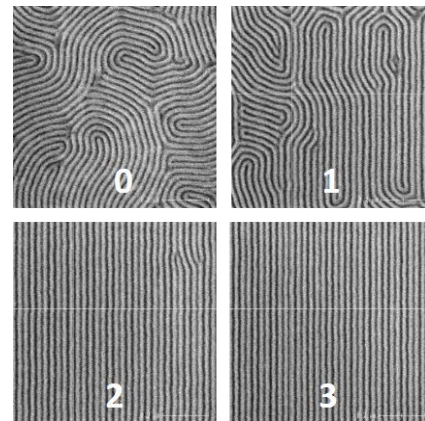


Figure 4. Evaluation of BCP assembly. A score of 0 was assigned to random orientation and 3 to perfectly aligned BCP domains.

good alignment of the BCP was 12.9nm (0.46L<sub>0</sub>). Below this value, the photoresist lines presented poor quality or were etched completely and therefore lacked a guiding stripe. A high degree of order can be achieved at W values around 0.6L<sub>0</sub>, which according to theoretical work, leads to straight profiles of the BCP throughout the film thickness[5]. Good registration with the underlying chemical pattern can be observed until W=0.9L<sub>0</sub>. Theoretical and experimental work indicates that as W approaches L<sub>0</sub>, diverse morphologies and three-dimensional structures may be formed even when alignment is observed at the top surface. This is undesirable when doing pattern transfer to the under layers, since different populations of CD may be formed. On the other end of the CD values, when W=L<sub>0</sub>, all order is lost and fingerprint-like structures are observed. For a 2X feature multiplication factor, Detcheverry and Liu reported that when a slightly preferential brush is used in the backfill regions, perpendicular orientation of the BCP domains is obtained in the range 0.25dW/L<sub>0</sub>d0.75, for several affinities of the guiding stripe.[9] Interestingly, mixed or non-identified morphologies were observed at W/L<sub>0</sub>=1 for almost any affinity of the guiding stripe that was explored. These observations were supported by Liu and Ramirez, who proved that for 4X density multiplication, when the ratio W/L<sub>0</sub> approaches 1, defects start forming until fingerprint like structures are obtained for specific chemistries.[5] The results reported in this study are in good agreement with previous work.

Furthermore, the response of different batches of BCP to changes in W was analyzed in a more detailed manner. For this study, a focus exposure matrix (FEM) was exposed and trim etched as

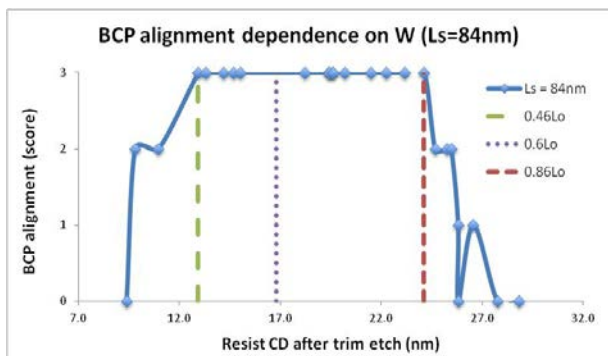


Figure 5. Process window for BCP assembly for 3X feature multiplication ( $L_s=84\text{nm}$  and  $L_o=28\text{nm}$ ).

described previously. The BCP assembly was investigated on large inspection blocks with  $L_s=84\text{nm}$ , available on the reticle. A total of  $62.5\mu\text{m}^2$  (10 SEM images at low magnification) were analyzed for each of the 11 available CD values. The response of different batches of BCP with the same  $L_o$  (28nm) was evaluated using the same scheme shown in Figure 4. Figure 6 shows the percentage of defect-free images (only score 3), and does not include the images that presented single defects or fingerprints (lower scores). For the three polymers, a lack of order can be seen at the low end of the  $W$  range. This may be due to irregular resist profiles after etching. At  $W=15.6\text{nm}$ , while defects were captured, the majority of the area on these fields presented good alignment of the BCP (score 2 or 3). If  $W$  is further decreased, large defect clusters are formed until random orientation is captured for all BCP batches. When  $W=L_o$ , the response of the three polymers is in good agreement with Figure 5. The present results show that subtle differences in the BCP formulation will impact the assembly process. A more detailed study is currently ongoing. This dependence becomes more evident when using uniform wafers. Three samples exposed at best dose/focus conditions, and processed as described previously, were coated with the different BCPs. After PMMA removal, SEM inspection was performed and, again,  $62.5\mu\text{m}^2/\text{die}$  were imaged on the main  $x$  and  $y$ -axis. The reported results in Figure 7 correspond to the number of images (out of 10) that received a score of 3. Two BCP batches, AZEMBLY™ PME312 and AZEMBLY™ PME120 did not generate any defects, while AZEMBLY™ PME252 formed defects randomly located on the wafer. An increasing sensitivity to edge effects can be observed from Figure 7a to 7c where the fields with defects are marked with an “X”. Samples a) and b) were able to heal most of the substrate non-uniformities. However, AZEMBLY™ PME120 shows a larger response to

differences on the chemical patterns. However, more information regarding the formulation is required to fully understand this behavior. In summary, control of the BCP natural periodicity is not enough to ensure reproducibility between batches during the DSA process. Subtle differences in BCP chemical composition may impact the process window for DSA and the ability of the BCP to heal some defects coming from the chemical pattern fabrication.

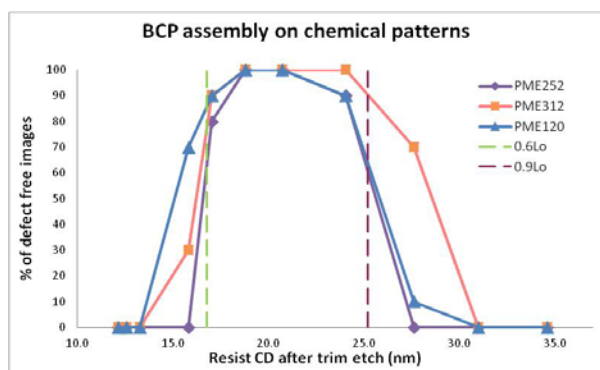


Figure 6. 3X density multiplication process window for 3 batches of BCP with  $L_o=28\text{nm}$ .

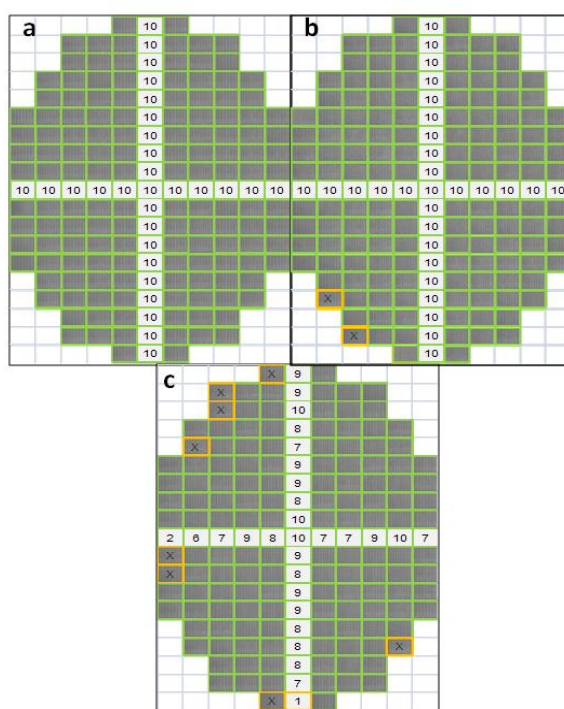


Figure 7. BCP assembly on uniform wafers for 3 different BCP batches: a) AZEMBLY™ PME312, b) AZEMBLY™ PME120, and c) AZEMBLY™ PME252. The numbers on the  $x$  and  $y$ -axis correspond to the number of images with score 3 (out of 10 images).

Last, the traditional inspection method used by the lithographic industry, which relies on single images at high magnification, does not provide enough information when evaluating DSA

of BCP. Single images at high magnification may not be representative of the full sample, since defects generate at random locations. Therefore, a more thorough evaluation is needed if optical inspection is not performed on the sample. Figure 8 shows the assessment of several conditions on the sample, where the same method was applied. The number of defect-free images (out of 10 images taken) is reported as a function of dose and focus. On this figure, the transition from perfectly aligned structures to random orientation can be appreciated, allowing the establishment of a more complete process window.

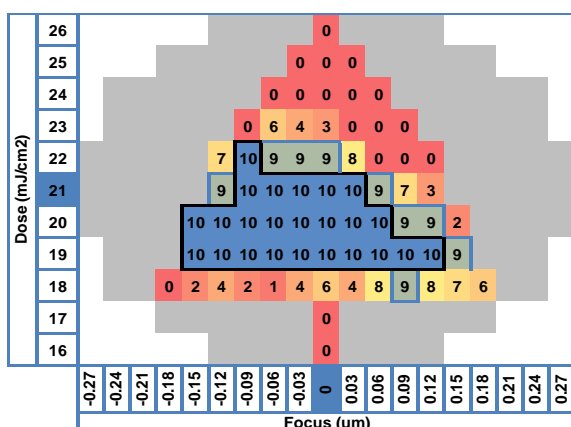


Figure 8. 3X density multiplication process window for AZEMBL<sup>TM</sup> PME312. The number of defect-free images is reported as a function of dose and focus (out of 10 images).

#### 4. Conclusions

For a given chemistry, the geometry of the chemical patterns will determine the type of morphology and its orientation during the assembly process. In the current study, for 3X feature multiplication, it has been shown that for a range of  $0.46L_0 < W < 0.9L_0$ , high degree of perfection can be achieved. The formulation of the BCP may have an impact on the process window for DSA. Additionally, a new inspection method to evaluate the DSA of BCP that provides the necessary information to establish a window for this process has been proposed. Currently, process parameters and alternative materials are being explored at imec to gain a deep understanding of the assembly process and establish a process window for implementation of DSA in high volume manufacture.

#### 5. Acknowledgements

The authors would like to thank Todd Younkin, from Intel Corporation, for helpful discussions. BT Chan is acknowledged for developing the plasma etching recipes and Samuel Suhard for support with the resist strip recipes. The

authors would also like to thank Ihsan Simms and Shane O'Neill, from Tokyo Electron, for their support with hardware-related questions.

#### 6. References

- International Technology Roadmap for Semiconductors: Lithography, 2010
- Rincon Delgadillo PA, Gronheid R, Thode CJ, Wu H, Cao Y, Neisser M, Somervell M, Nafus K, Nealey PF: Implementation of a chemo-epitaxy flow for directed self-assembly on 300mm wafer processing equipment, In preparation, 2012,
- Bencher C, Smith J, Miaoa L, Caia C, Chena Y, Cheng JY, Sanders DP, Tjioeb M, D. TH, Holmes S, Hinsberg WD: Self-assembly patterning for sub-15nm half-pitch: A transition from lab to fab, *Proc. SPIE*, **2011**, 7970,
- Rincon Delgadillo PA, Gronheid R, Thode CJ, Wu HW, Cao Y, Somervell M, Nafus K, Nealey PF: All track directed self-assembly of block copolymers: Process flow and origin of defects. *Proc. SPIE* **8323** (2012), 83230D.
- Liu C-C, Ramirez Hernandez A, Yoshita H, Kang H, Han E, Padma Gopalan, dePablo JJ, Nealey PF: Free energy minimization for directed self-assembly of block copolymers with density multiplication. In preparation,
- Edwards EW, Montague MF, Solak HH, Hawker CJ, Nealey PF: Precise control over molecular dimensions of block-copolymer domains using the interfacial energy of chemically nanopatterned substrates. *Advanced Materials*, **16** (2004), 1315.
- Liu C-C, Han E, Onses MS, Thode CJ, Ji S, Gopalan P, Nealey PF: Fabrication of lithographically defined chemically patterned polymer brushes and mats. *Macromolecules*, **44** (2011), 1876-1885.
- Chi-Chun L, Nealey PF, Raub AK, Hakeem PJ, Brueck SRJ, Eungnak H, Gopalan P: Integration of block copolymer directed assembly with 193 immersion lithography. *J. Vacuum Sci. Technol. B (Microelectronics and Nanometer Structures)* **2010**, 28
- Detcheverry FA, Liu G, Nealey PF, de Pablo JJ: Interpolation in the directed assembly of block copolymers on nanopatterned substrates: Simulation and experiments. *Macromolecules*, **43** (2010), 3446-3454.
- Liu GL, Kang HM, Craig GSW, Detcheverry F, de Pablo JJ, Nealey PF, Tada Y, Yoshida H: Cross-sectional imaging of block copolymer thin films on chemically patterned surfaces. *J. Photopolym. Sci. Technol.*, **23** (2010), 149-154.
- Liu C-C, Thode CJ, Rincon Delgadillo PA, Craig GSW, Nealey PF, Gronheid R: Towards an all-track 300mm process for directed self-assembly, *J. Vac. Sci. Technol. B*, **2011**, 29,